PhotoniX

Ultrafast (600 ps) α-ray scintillators

Richeng Lin[1†], Yanming Zhu[1†], Liang Chen[2†], Wei Zheng[1*] , Mengxuan Xu[3], Jinlu Ruan[2], Renfu Li[4], Titao Li[1], Zhuogeng Lin[1], Lu Cheng[1], Ying Ding[1], Feng Huang[1*] and Xiaoping Ouyang[2,5*]

*Correspondence:
zhengw37@mail.sysu.edu.cn;
huangfeng@mail.sysu.edu.cn;
oyxp2003@aliyun.com
†Richeng Lin, Yanming Zhu and Liang Chen contributed equally　this work.
[1] State Key Laboratory of Optoelectronic Materials and Technologies, School of Materials, Sun Yat-Sen University, Guangzhou 510275, China
[2] State Key Laboratory of Intense Pulsed Radiation Simulation and Effect and Radiation Detection Research Center, Northwest Institute of Nuclear Technology, Xi'an 710024, China
Full list of author information is available at the end of the article

Abstract

Large-size scintillators with high efficiency and ultrafast radiation fluorescence have shown more potential in the applications to ionizing radiation detection of medical diagnosis, nuclear control and high-energy physics. Currently, although traditional scintillators have made tremendous progress in scintillation efficiency, there are still challenges left in fluorescence lifetime. Faced with that problem, we adopted 2-inch ZnO as the substrate and doped gallium as activator to realize an ultrafast fluorescence excited by α-ray, of which the decay time is only 600 ps that is the shortest scintillation decay time reported so far. The results show that the shallow donor related with gallium not only effectively suppresses band-edge self-absorption, but makes ultrafast radiation possible, which gets gallium-doped ZnO as a potential scintillator for high-quality ultrafast dynamic imaging proved.

Keywords: Scintillators, Gallium doped zinc oxide, Decay time, Radioluminescence

Introduction

In recent years, high-energy ray imaging has been widely used in the fields of medical diagnosis, security and scientific research [1–3]. Time response and light yield are considered to be the most important evaluation indices of dynamic imaging quality. In general, high-energy ray imaging relies on scintillators that can convert high-energy rays into visible or ultraviolet photons [4, 5], which gives a privilege to the fluorescence decay time and light yield of scintillators to determine the quality of high-energy ray imaging.

Due to the high light yield, thallium-doped cesium iodide is widely used in various situations. However, its long fluorescence decay time that is almost up to 1000 ns limits its application in some fields, such as ultrafast dynamic probing. Therefore, finding a scintillator with ultrafast luminescence characteristics becomes a research subject attracting much attention. Recently, various perovskites have been taken as focus due to their low preparation cost and excellent emission performance [6–12]. Huang et al. reported an all-inorganic perovskite ($CsPbX_3$, $X = Cl$, Br, I) nanocrystalline scintillator with a luminescence decay time of 44 ns [13]. Yang et al. synthesized a kind of nontoxic double perovskite ($Cs_2Ag_{0.6}Na_{0.4}In_{0.85}Bi_{0.15}Cl_6$) in the research where the fabricated sample was ground into powder and pressed into a 2-inch slice with the light yield commensurate with that of commercial scintillator thallium-doped cesium iodide. What's more, this double perovskite shows a microsecond fluorescence decay time [14]. Compared

with other perovskites, the near-band-edge (NBE) radiation of gallium-doped zinc oxide (ZnO:Ga) has a sub-nanosecond ultrafast time response, which makes it a promising candidate material for detecting ultrafast signals [15–22]. In addition, its fluorescence emission of defects has been greatly inhibited by the maturing hydrothermal crystal growth technology, which promotes the development of large-size ZnO:Ga single-crystal scintillators.

In this work, we grow a 2-inch ZnO:Ga single crystal wafer via hydrothermal method. In the light of the band-edge radiation characteristics of ZnO:Ga, that is, low light yield and fast response, we set up an alpha-ray excited single-particle time-resolved emission spectrum measurement system, based on which the decay time of band-edge fluorescence of ZnO:Ga single crystal is directly obtained. In addition, according to a high spatial resolution (2.63 lp mm^{-1}) at high X-ray dose, the prospect of ZnO:Ga single crystal as a promising scintillator has been suggested and proved.

Materials and methods

ZnO:Ga single crystal growth

We grow a high-quality ZnO:Ga single crystal via hydrothermal method. A large-size autoclave made of high-hardness Ni–Cr alloy is taken as the reaction vessel for ZnO:Ga fabrication, which can be divided into growth zone and dissolution zone. In the growth zone, high-quality ZnO seed crystals are distributed there. In the dissolution zone, Zinc oxide and gallium oxide powders sintered at high temperature are stacked with a mass ratio of 99:1. Fill the autoclave with an aqueous solution containing mineralizer, and then heat the growth zone to 400℃ with a temperature gap kept between the two zones all along, that is, the temperature of dissolution zone is 20 ~ 40℃ higher than that of growth zone. Besides, during the whole growing process, the pressure in autoclave is maintained at 80–100 MPa. Under this condition of both high temperature and pressure, the mixed powder in dissolution zone will dissolve into the solution, and then the bottom solution will rise and inflow the top growth zone due to the existence of temperature difference. Finally, the top solution is supersaturated, and then ZnO:Ga begins to grow gradually.

Material characterization

All the data and spectra of this work are achieved through different devices or based on various systems. The XRD measurement in Figure S1 takes use of an Empyrean diffractometer with Cu-K$_\alpha$ ($\lambda = 1.5406$Å). The ultraviolet photoluminescence (UV-PL) spectrum in Fig. 1(c) is measured via a self-built fluorescence spectrum measurement system which is equipped with a 266 nm pulsed laser and a spectrometer (QE65 Pro, Ocean Optics) with wide detection range from 200 to 900 nm. The transmission spectrum of ZnO:Ga is performed via ultraviolet spectrophotometer (SHIMADZU UV-3600 Plus) in the range from 300 to 800 nm. The infrared absorption spectrum measured in Figure S3 is achieved by Fourier-transform infrared spectroscopy (IRAffinity-1S). The Raman spectrum in Figure S4 employs the Renishaw inVia reflex Raman spectroscopy. The X-ray photoelectron spectrum in Figure S5 are plotted by Thermo fisher ESCLAB XI of Songshan Lake Materials Laboratory. The AFM topographic image in Figure S6 is scanned with CSPM5500. The HRTEM measured are obtained by FEI, Talos F200 S.
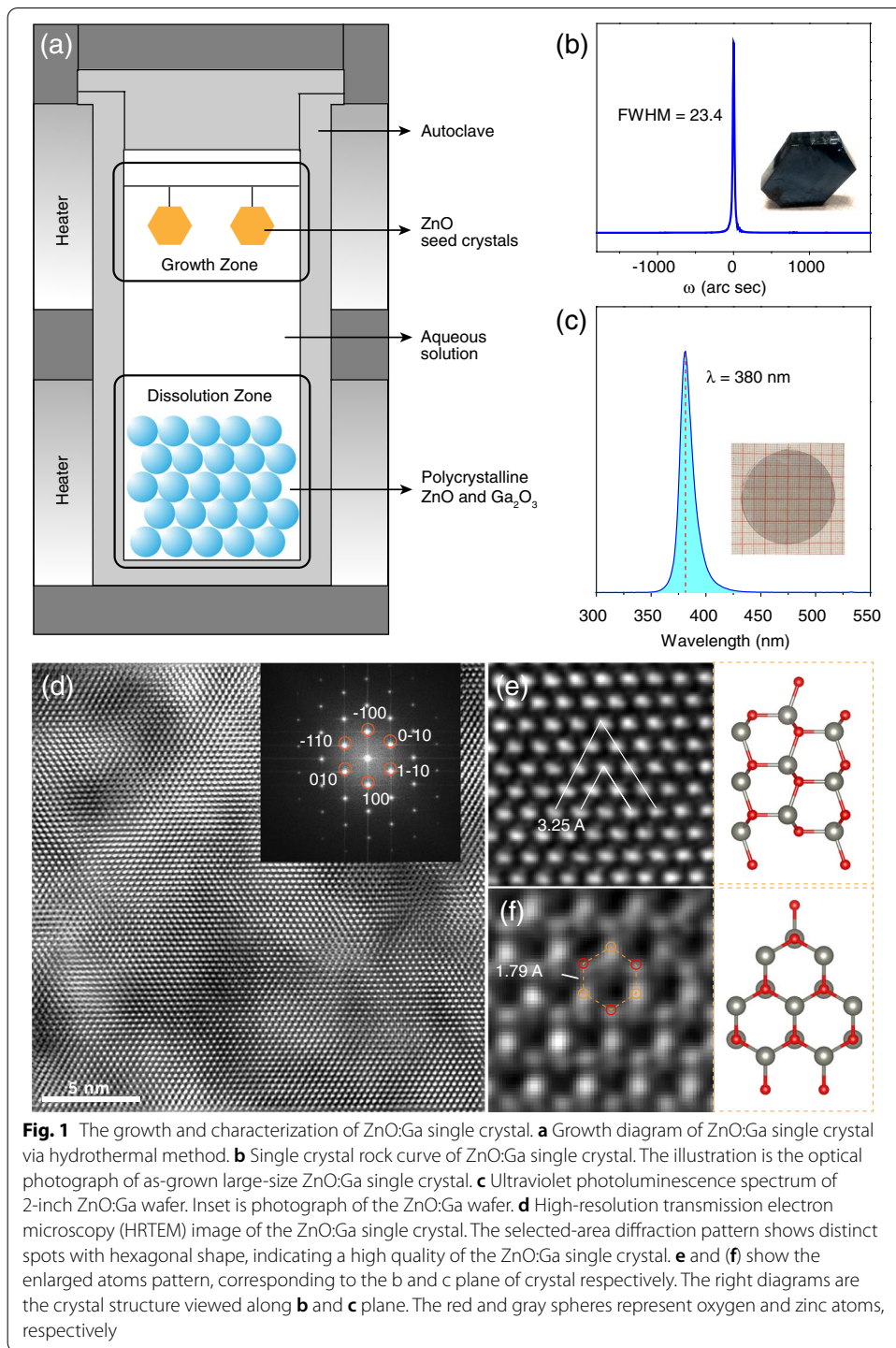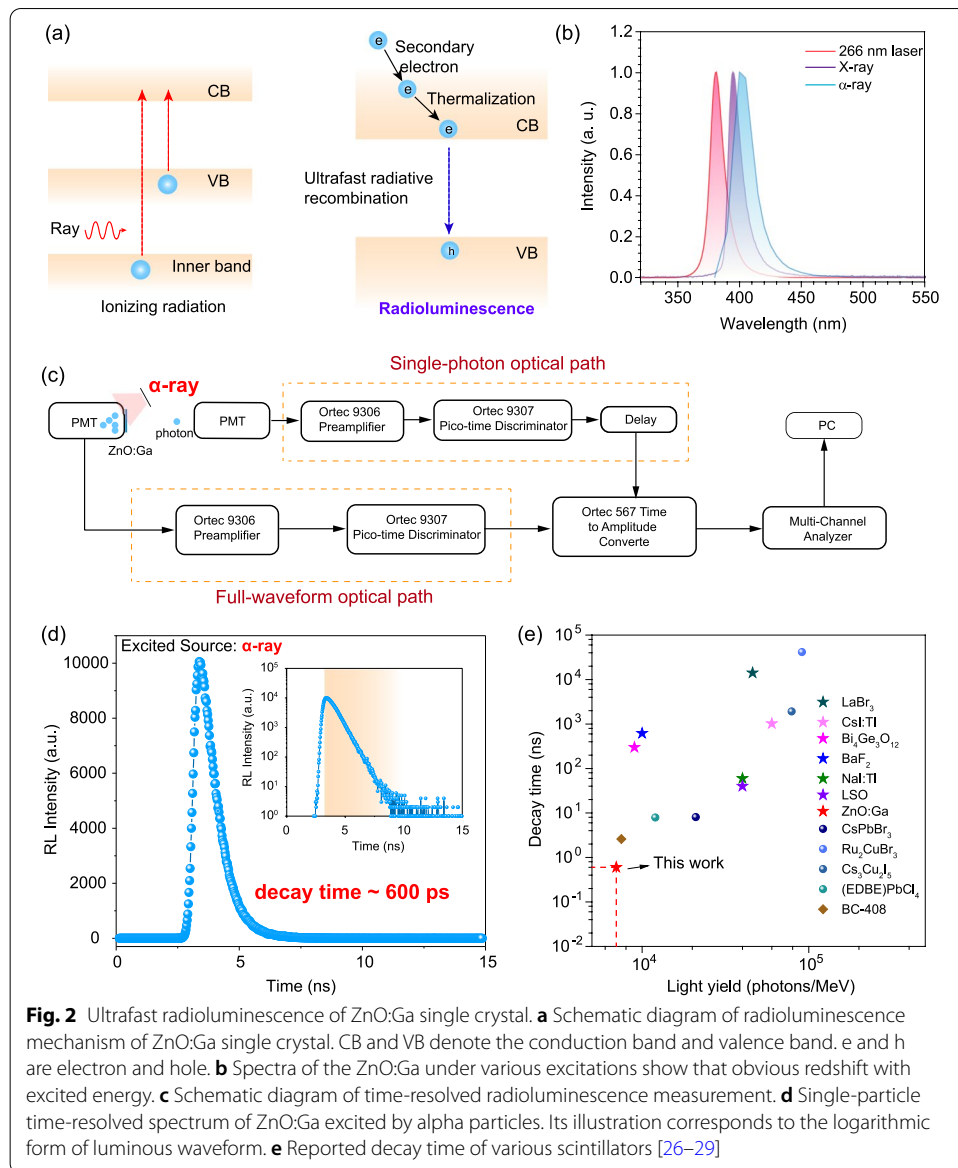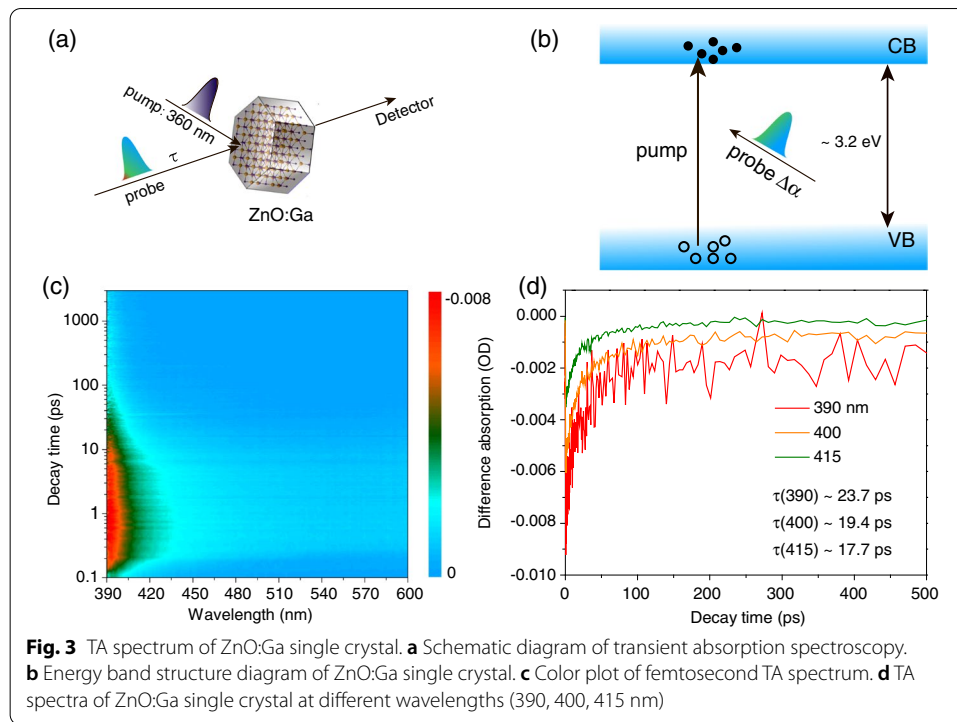
Fig. 1 The growth and characterization of ZnO:Ga single crystal. **a** Growth diagram of ZnO:Ga single crystal via hydrothermal method. **b** Single crystal rock curve of ZnO:Ga single crystal. The illustration is the optical photograph of as-grown large-size ZnO:Ga single crystal. **c** Ultraviolet photoluminescence spectrum of 2-inch ZnO:Ga wafer. Inset is photograph of the ZnO:Ga wafer. **d** High-resolution transmission electron microscopy (HRTEM) image of the ZnO:Ga single crystal. The selected-area diffraction pattern shows distinct spots with hexagonal shape, indicating a high quality of the ZnO:Ga single crystal. **e** and (**f**) show the enlarged atoms pattern, corresponding to the b and c plane of crystal respectively. The right diagrams are the crystal structure viewed along **b** and **c** plane. The red and gray spheres represent oxygen and zinc atoms, respectively

Time-resolved radioluminescence measurement

The time-resolved radiation decay time is measured by a single-particle time-resolved emission spectroscopy (SP-TES) system. The schematic diagram of measurement is plotted in Fig. 2. The system uses single-photon counting technology (SPCT) to collect signals and consists of two detection subsystems, the full-wave path and the single-photon

Fig. 2 Ultrafast radioluminescence of ZnO:Ga single crystal. **a** Schematic diagram of radioluminescence mechanism of ZnO:Ga single crystal. CB and VB denote the conduction band and valence band. e and h are electron and hole. **b** Spectra of the ZnO:Ga under various excitations show that obvious redshift with excited energy. **c** Schematic diagram of time-resolved radioluminescence measurement. **d** Single-particle time-resolved spectrum of ZnO:Ga excited by alpha particles. Its illustration corresponds to the logarithmic form of luminous waveform. **e** Reported decay time of various scintillators [26–29]

path. The full-wave channel output signal is relatively stable, so the signal recorded in multiple channels depends on the single-photon signal. We can equate each single photon signal as randomly extracting a photon from a single alpha particle excitation process, so the single photon signal represents the luminescence of the sample. A high-gain PMT (ET 9813) is set close to the ZnO:Ga wafer to collect photons as the zero-time signal as many as possible. Another fast-response microchannel plant PMT (MCP-PMT, Hamamatsu R3809U-50) is kept far away from the sample to collect single-photon signal. When the single-photon signal is transmitted to Ortec 567 time-to-amplitude converter, a luminous waveform with a corresponding wavelength of 394 nm can be obtained. Place a Newport Oriel 74,125 Cornerstone 260 UV–Vis-1-4 m Monochromator before MCP-PMT, and then the color plot of Time-resolved emission spectrum containing both spectral and temporal information of ZnO:Ga single crystal can be achieved.

Fig. 3 TA spectrum of ZnO:Ga single crystal. **a** Schematic diagram of transient absorption spectroscopy. **b** Energy band structure diagram of ZnO:Ga single crystal. **c** Color plot of femtosecond TA spectrum. **d** TA spectra of ZnO:Ga single crystal at different wavelengths (390, 400, 415 nm)

Transient absorption spectrum measurement

The color plot of femtosecond TA spectrum is shown in Fig. 3(c), where the probed absorption coefficient is collected by a transient absorption spectrometer (Helios, Ultra-fast System) with a wide detection range from 390 to 1600 nm. The pumped femto-second laser whose model is Spitfire is from Spectra-Physics. With the help of optical parametric amplifier, the wavelength range of that pump laser can be adjusted casually between 300 to 2400 nm.

X-ray imaging measurement

The sketch map of X-ray imaging measurement is shown in Fig. 5(a). Excited fluorescence is recorded by a camera through a mirror. Here, the adopted X-ray source is TUB00140-W06 of Moxtek whose maximum power is 12 W and that can be tuned via changing voltage or current. The X-ray dose rate corresponding to different power is detected by radiation power meter (Didotime-r, QUART). The camera is iKon-M, ANDOR, which is equipped with UV-enhanced lens (Nikon Rayfact PF10545MF-UV). During the measurement, the shutter was normally open. The adopted line pair test pattern (70,358, QUART) is plotted in Figure S8(a), whose material is lead foil, thickness is 0.03 mm, and maximum line pairs were 20 lp mm^{-1}.

Results and discussion

In this work, the crystal growth method we use is an improving hydrothermal method. As we all know, the advantage of the hydrothermal method is that it is easy to achieve low temperature equilibrium crystal growth, which is very critical to obtain crystals with excellent crystal quality and uniform doping. The principle of crystal growth is

shown in Fig. 1(a), and the details of growth process are described in the Methods section. The illustration in Fig. 1(b) shows the photograph of the large-size ZnO:Ga single crystal whose appearance is a dark blue hexagon. Its surface topography and X-ray diffraction (XRD) patterns are described in supporting information [23]. According to the single crystal rocking curve plotted in Fig. 1(b), the full width at half maxima (FWHM) of ZnO:Ga single crystal is 23.4 arc sec, which is much lower than that of ZnO:Ga film reported so far, [24–26] indicating that the ZnO:Ga single crystal fabricated by hydrothermal method has high lattice integrity and low defect density. After wire cutting and polishing, a 2-inch ZnO:Ga wafer is obtained with its optical photograph shown in the illustration of Fig. 1(c). Via a 266 nm pulsed laser with a frequency of 2 MHz, the ultraviolet photoluminescence (UV-PL) spectrum is obtained and displayed in Fig. 1(c), where only a single emission peak is observed with a corresponding wavelength at 380 nm [27]. In Fig. 1(d), The crystal structure of the obtained ZnO:Ga was characterized by HRTEM, in which the selected area diffraction showed only one set of lattices of ZnO, which could be attributed to the small amount of doping (ppm level) of Ga. In this work, the carrier concentration of the ZnO:Ga single crystal is about 1018 cm-3. In addition, the complete ZnO lattice also illustrates the high crystalline quality of the crystal, which enables the crystal to have a high light yield. The enlarged atoms patterns (Fig. 1(e) and (f)) corresponding to the **b** and **c** plane of crystal respectively show consistency with crystal structure. The results show that the ZnO:Ga single crystal grown by hydrothermal method has high crystal quality.

The mechanism of radioluminescence (RL) of ZnO:Ga single crystal is plotted in Fig. 2(a). Once ionizing radiation (alpha-ray and X-ray) reaches ZnO:Ga single crystal, a large number of inner-shell electrons and valence electrons will be pumped into conduction band and even vacuum-energy level and thus generate extensive hot electrons and high-energy holes. At the same time, a great number of secondary electrons are generated by inelastic electron scattering and auger process to achieve low-energy carrier multiplication. These low-energy carriers are thermalized in an ultra-short time scale and then trapped by luminescent center. Finally, abundant ultraviolet photons will be released from lattice. Under different excitations, the spectra of ZnO:Ga single crystal was shown in Fig. 2(b). When the 266 nm laser is used as excitation, the peak of spectrum is at ~ 380 nm, which corresponds to the band gap of ZnO. The shape of emission peak is not Gaussian, but has a low-energy shoulder, which can be attributed to doping Ga atoms. It is also noticed a red-shift of the emission peak with increasing excitation energy. We believe that the reason for this phenomenon is that the near-band-edge (NBE) emission of crystals is difficult to avoid the effect of self-absorption. In addition, under the excitation of x-ray and α-ray, the luminescence intensity of ZnO is smaller, and the effect of self-absorption is more obvious, which is the reason for the red shift of the emission peak. This explains why the intrinsic ZnO has almost no fluorescence under the excitation of high-energy rays.
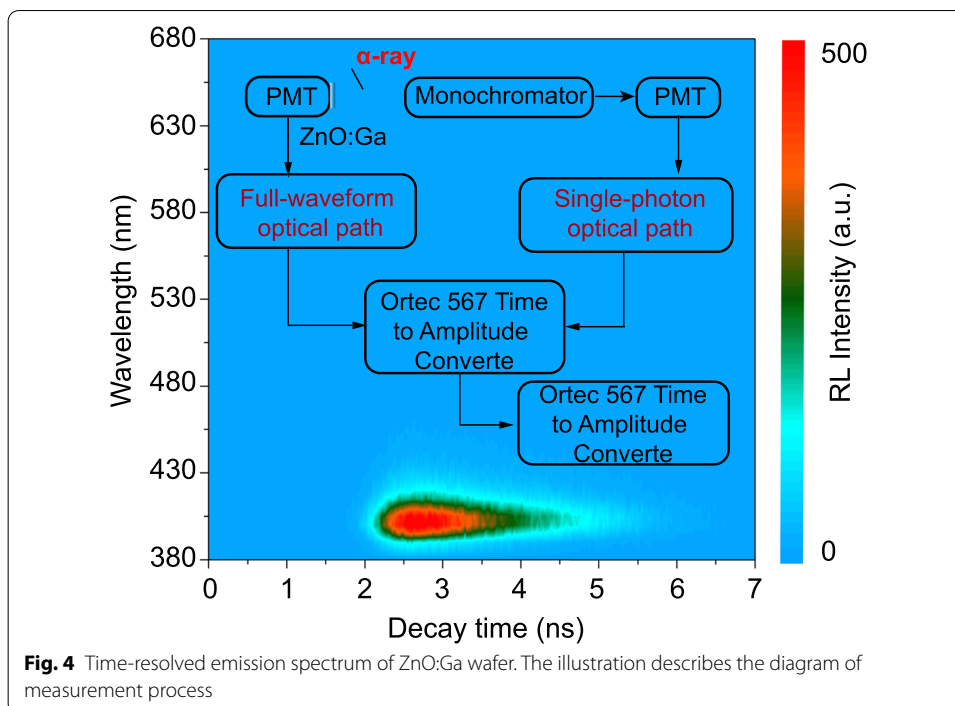
As we elaborated above, the decay time of scintillator is one of the critical factors to affect the quality of high-energy ray imaging. Collecting luminous waveform via oscilloscope is usually the simplest pattern to obtain the information about time response. However, ZnO:Ga single crystal is always considered as a scintillator with low light yield, which suggests that the signal-to-noise ratio (SNR) of collected luminous waveform is

too low to distinguish the signal from the noise. In order to overcome this defect, we designed a time-resolved radioluminescence measurement system based on single-photon counting technology (SPCT), whose detailed diagram is shown in Fig. 2(c) [28, 29]. One high-gain photomultiplier tube (PMT) is set close to the ZnO:Ga wafer to collect photons as the zero-time signal as many as possible. Another fast-response PMT coupled with monochromator is kept far away from the sample to collect single-photon signal. When the single-photon signal is transmitted to Ortec 567 time to amplitude converter, a luminous waveform with a corresponding wavelength of 394 nm can be obtained. Here, we use alpha-particles emitted from ^{241}Am source (11000 Bq) to bombard ZnO:Ga wafer. The luminous waveform of ZnO:Ga single crystal is plotted in Fig. 2(d), where the number of emitted ultraviolet photons whose energy is 3.15 eV begins to attenuate in the form of single exponential function after a short-time increasing process. Figure 2d shows the typical waveform of a ZnO sample obtained by the SPCT. The superposition of coincidence events is achieved by greatly eliminating the interference of noise. The rise time of the luminescence in Fig. 2d is only 0.38 ns, and the tail of the waveform achieves single exponential decay within more than three orders of magnitude, indicating that the results truly show the time response characteristics of the sample. The decay time constant is 0.64 ns, indicating that our system can accurately measure the luminescence decay time of scintillators with weak luminescence and fast response. By fitting the afterglow curve with single e exponential function that $y = A * \exp(-x/\tau) + y_0$, the decay time τ of ZnO:Ga single crystal is obtained, that is almost 600 ps.

The performance of conventional inorganic scintillators and emerging perovskite scintillators was statistically shown in Fig. 2e [30–33]. At the same time, the properties of similar ZnO and its doped materials, such as ZnO:In, ZnO:Sc and ZnO:Cd were also systematically observed [34, 35]. It is found that ZnO:Ga material has obvious advantages in luminescence yield. To perform scintillation tests on natural undoped ZnO and ZnO:Ga single crystals, it found that almost no scintillation was observed in ZnO, which may be due to the fact that the emission and absorption of ZnO are almost overlapping, leading to fatal self-absorption of scintillation, which is inherently inefficient. In contrast, the introduction of Ga element makes the emission avoid the self-absorption, so ZnO:Ga has a higher light yield. Furthermore, Ga doping did not lead to additional emission peaks, and the near-band-edge emission still dominated as the fast component, which had advantages over ZnO doped with other elements.

To understanding the ultrafast RL radiation mechanism, we perform a transient absorption (TA) spectroscopy to measure the excited state of ZnO:Ga, of which the corresponding schematic diagram is displayed in Fig. 3(a). The energy band structure of ZnO:Ga single crystal is shown in Fig. 3(b). During the experiment, a Femtosecond laser at 360 nm with a pulse width of 120 fs is used to excite the sample, and then the relative changes of absorption of supercontinuum probe pulse from 390 to 600 nm after a certain decay time are recorded via Helios, a commercialized transient absorption spectrometer from Ultrafast System.

For the TA spectrum, the photon energy range absorbed by different processes is different, so the absorption peaks at different wavelength positions on the absorption spectrum with a fixed relaxation time can be distinguished. In the TA spectrum of

Fig. 4 Time-resolved emission spectrum of ZnO:Ga wafer. The illustration describes the diagram of measurement process

ZnO:Ga single crystal, the bleaching peak at 390 nm is due to the reduction of ground-state particles due to bandgap transitions, shown in Fig. 3(c). In the whole spectral range (390, 400 and 415 nm), there are no other absorption peaks, which indicates that the doping of Ga into ZnO does not cause additional excited-state absorption and photoproduct absorption that delay the decay time. This is crucial for obtaining ultra-fast fluorescence of ZnO:Ga single crystals. Then we extract three curves at different wavelengths from Fig. 3(c) and get them fitted with a single e exponential function, from which the decay time corresponding to 390, 400 and 415 nm is obtained as 23.7, 19.4 and 17.7 ps respectively. On the basis of those results, the clean near-band-edge emission that verifed by the measured TA spectrum leads the ultrafast fluorescence of ZnO:Ga single crystals.

The radiation decay time is measured by a single-particle time-resolved emission spectroscopy (SP-TES) system, which has the advantage of avoiding distortion due to weak signals and having fast time response performance. The principle of the SP-TES system is briefly described in Fig. 4 inset. In order to obtain the spectral and temporal information of ZnO:Ga near-band-edge luminescence at the same time, we added a monochromator in front of the single-photon optical path, as shown in the illustration of Fig. 4. A single-photon counting technology is adopted to collect the luminous waveform every 5 nm in the range of 380–700 nm, and the measurement result is shown in Fig. 4. By integrating time, the RL spectrum of ZnO:Ga wafer is shown in Fig. 2(b), where the emission peak is located at 394 nm. An obvious difference between the RL spectrum and the UV-PL spectrum can be observed. The wavelength corresponding photoluminescence peak excited by 266 nm pulse laser is 380 nm, while that of radioluminescence peak excited by X-ray is 394 nm, which is originated from the strong self-absorption of ZnO:Ga single crystal. Since the interaction between 266 nm pulse laser and ZnO:Ga

wafer mainly focuses on surface, excited fluorescence is easy to escape from lattice, but the situation is different as the interaction between high-energy ray and the sample is concentrated in the interior of ZnO:Ga wafer due to the large penetration depth of high-energy ray, which means the excited fluorescence has to pass through the sample to get emitted. In addition, there is a strong self-absorption for the near-band-edge radiation in ZnO:Ga single crystal, and the absorption coefficient increases significantly with the decrease of wavelength. In Fig. 4, the ZnO:Ga single crystal also shows a ultrafast RL with 3 ns decay time.

As well known, the ionizing radiation detection, including neutrons, alpha rays and X-rays, has important applications in medical diagnosis, high-energy physics and nuclear energy control. Among them, fast X-ray imaging is very important in the pulsed X-ray radiation field generated by radiation events such as high-temperature dense plasma, and it is also a technology that needs to be solved urgently. In this part, we discuss the performance of ZnO:Ga crystal in X-ray imaging, the purpose is to verify the ability of ZnO:Ga crystal in X-ray imaging, combined with the fast luminescence of the crystal to illustrate its performance in the above-mentioned fast X-ray imaging application. The spatial resolution of a scintillator is an important factor for realizing the dynamic imaging of ultrafast process as well as a pivotal index to evaluate the quality of high-energy ray imaging. Figure 5(a) is the schematic diagram of X-ray imaging system, where the imaging object is placed between the X-ray source and ZnO:Ga scintillator but close to the latter. Under X-ray irradiation, the fluorescence emitted from the unshielded ZnO:Ga wafer is received by the ultraviolet-enhanced camera through reflector. Here, we took a measurement of the spatial resolution of ZnO:Ga scintillator under different X-ray doses, during which the exposure time was 10 s, and the results are shown in Fig. 5(b) to (f). Figure S8(a) is the optical photograph of that line pair test pattern, which distributes sawtooth with different densities in different areas. When the X-ray dose rate is 3.15 mGy/s, the radiograph spatial resolution of ZnO:Ga scintillator is 3.15 lp mm^{-1}; and when the X-ray dose rate is up to 5.65 mGy/s, the radiograph spatial resolution of ZnO:Ga scintillator is 4.5 lp mm^{-1}. We also extracted the RL intensity of region A and B at different X-ray dose rate, and results were present in Figure S8(b), where the RL intensity is nearly proportional to radiation dose rate. This conclusion is consistent with the rule in Figure S8(b), that with the decrease of X-ray dose, the RL intensity decreases linear. It is also clear that the detection limit is almost 3.15 mGy/s. Although ZnO:Ga is a kind of scintillator with low light yield, it still has a high spatial resolution under X-ray illumination with large dose rate. Figure S9 displays the X-ray imaging of integrated chip under the X-ray radiation dose rate of 29.13 mGy/s,[14] where various details with its pins included can be clearly observed in the X-ray imaging. All the findings above prove that ZnO:Ga single crystal is an excellent candidate scintillator to detect ultrafast dynamic process under large radiation doses.

Conclusions

In this work, we fabricate a high-quality ZnO:Ga single crystal with the diameter of 2 inches by hydrothermal method, and take a measurement on its RL spectrum where the RL peak is located at 394 nm. Besides, according to the time-resolved emission spectrum of ZnO:Ga single crystal, the ultrafast luminescent decay time
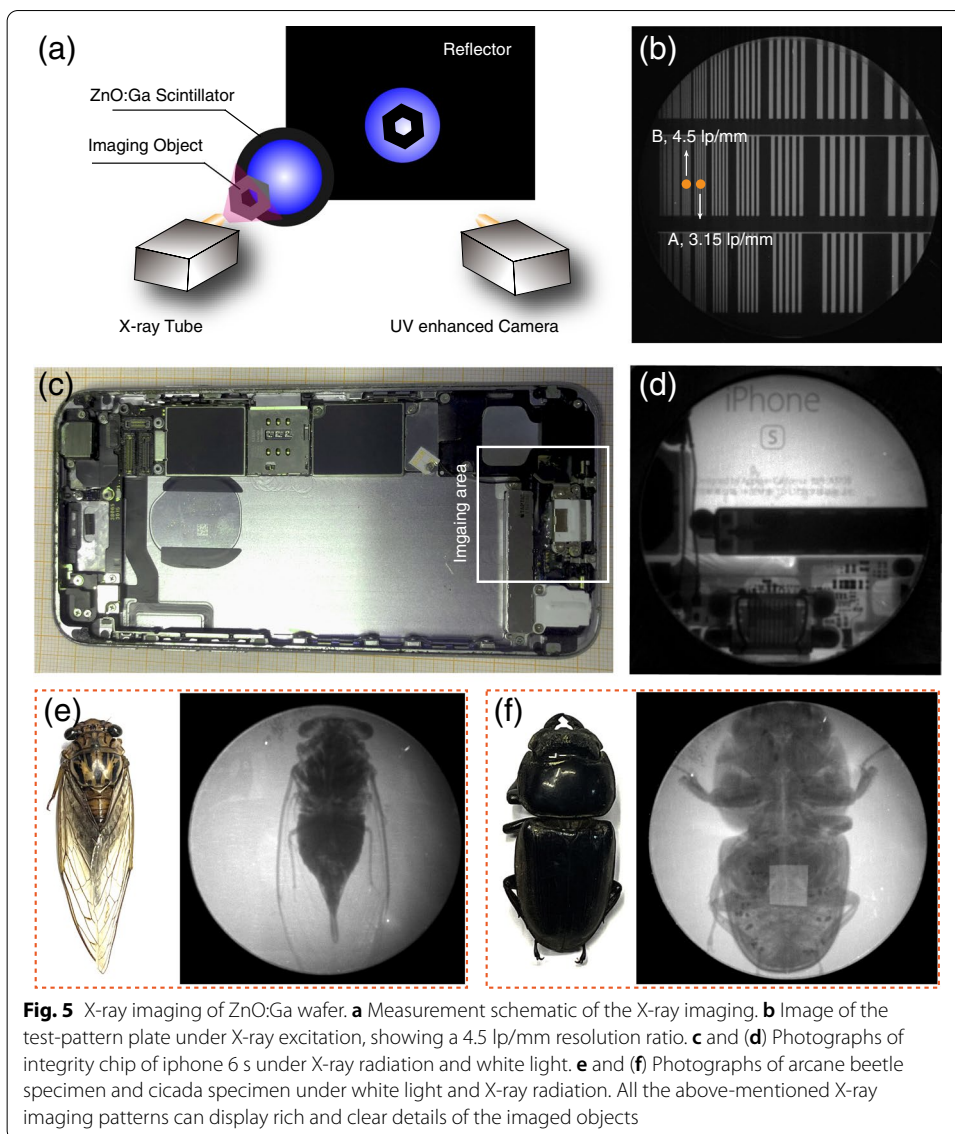
Fig. 5 X-ray imaging of ZnO:Ga wafer. **a** Measurement schematic of the X-ray imaging. **b** Image of the test-pattern plate under X-ray excitation, showing a 4.5 lp/mm resolution ratio. **c** and (**d**) Photographs of integrity chip of iphone 6 s under X-ray radiation and white light. **e** and (**f**) Photographs of arcane beetle specimen and cicada specimen under white light and X-ray radiation. All the above-mentioned X-ray imaging patterns can display rich and clear details of the imaged objects

excited by alpha particles is obtained as 600 ps. The spatial resolution and ultrafast luminescence characteristics of ZnO:Ga single crystal under high-dose X-ray irradiation indicate that ZnO:Ga single crystal is a potential scintillator for ultrafast dynamic imaging.

Abbreviations
ZnO: Zinc oxide; ZnO:Ga: Gallium-doped zinc oxide; UV-PL: Ultraviolet photoluminescence; MCP: Microchannel plant; PMT: Photomultiplier tube; XRD: X-ray diffraction; FWHM: Full width at half maxima; HRTEM: High-resolution transmission electron microscopy; SNR: Signal-to-noise ratio; RL: Radioluminescence; TA: Transient absorption.

Supplementary Information
The online version contains supplementary material available at https://doi.org/10.1186/s43074-022-00054-4.

Additional file 1. This supplementary information provides details on XRD, absorption spectrum, Ranman spectrum, XPS, AFM pattern, temperature-dependent PL and RL spectrum and X-ray images of the ZnO:Ga wafers.

Declarations

Ethics approval and consent to participate
Not applicable.

Competing interests
The authors declare no competing interests.

Author details
[1]State Key Laboratory of Optoelectronic Materials and Technologies, School of Materials, Sun Yat-Sen University, Guangzhou 510275, China. [2]State Key Laboratory of Intense Pulsed Radiation Simulation and Effect and Radiation Detection Research Center, Northwest Institute of Nuclear Technology, Xi'an 710024, China. [3]School of Nuclear Science and Technology, Xi'an Jiaotong University, Xi'an 710049, China. [4]CAS Key Laboratory of Design and Assembly of Functional Nanostructures, Fujian Key Laboratory of Nanomaterials, Fujian Institute of Research On the Structure of Matter, Chinese Academy of Sciences, Fuzhou 350002, China. [5]School of Materials Science and Engineering, Xiangtan University, Xiangtan 411105, China.

References
1. Grüneboom A, Kling L, Christiansen S, Mill L, Maier A, Engelke K, Quick HH, Schett G, Gunzer M. Next-generation imaging of the skeletal system and its blood supply. Nat Rev Rheumatol. 2019;15(9):533–49. https://doi.org/10.1038/s41584-019-0274-y.
2. Hachadorian RL, Bruza P, Jermyn M, Gladstone DJ, Pogue BW, Jarvis LA. Imaging radiation dose in breast radiotherapy by X-ray CT calibration of Cherenkov light. Nat Commun. 2020;11:2298. https://doi.org/10.1038/s41467-020-16031-z.
3. Lin R, Zheng W, Chen L, Zhu Y, Xu M, Ouyang X, Huang F. X-ray radiation excited ultralong (>20,000 seconds) intrinsic phosphorescence in aluminum nitride single-crystal scintillators. Nat Commun. 2020;11:4351. https://doi.org/10.1038/s41467-020-18221-1.
4. Blasse G. Scintillator materials. Chem Mater. 1994;6:1465–75. https://doi.org/10.1021/cm00045a002.
5. Rodnyi PA, Dorenbos P, Van Eijk CW. Energy loss in inorganic scintillators. Phys Stat Sol (b). 1995;187:15–29. https://doi.org/10.1002/pssb.2221870102.
6. Lin R, Guo Q, Zhu Q, Zhu Y, Zheng W, Huang F. All-Inorganic CsCu2I3 Single Crystal with High-PLQY (≈15.7%) Intrinsic White-Light Emission via Strongly Localized 1D Excitonic Recombination. Adv Mater. 2019;31–1905079. https://doi.org/10.1002/adma.201905079.
7. Zheng W, Huang F, Zheng R, Wu H. Low-dimensional structure vacuum-ultraviolet-sensitive (λ< 200 nm) photodetector with fast-response speed based on high-quality AlN micro/nanowire. Adv Mater. 2015;27:3921–7.
8. Xu LJ, Lin X, He Q, Worku M, Ma B. Highly efficient eco-friendly X-ray scintillators based on an organic manganese halide. Nat Commun. 2020;11:4329. https://doi.org/10.1038/s41467-020-18119-y.
9. Cho S, Kim S, Kim J, Jo Y, Ryu I, Hong S, Lee JJ, Cha S, Nam EB, Lee SU, Noh SK, Sam K, Kim H, Kwak J, Im H. Hybridisation of perovskite nanocrystals with organic molecules for highly efficient liquid scintillators. Light Sci Appl. 2020;9:156. https://doi.org/10.1038/s41377-020-00391-8.
10. Thirimanne HM, Jayawardena KDGI, Parnell AJ, Bandara RMI, Karalasingam A, Pani S, Huerdler JE, Lidzey DG, Tedde SF, Nisbet A, Mills CA, Silva SRP. High sensitivity organic inorganic hybrid X-ray detectors with direct transduction and broadband response. Nat Commun. 2018;9:2926. https://doi.org/10.1038/s41467-018-05301-6.
11. Zhao J, Zhao L, Deng Y, Xiao X, Ni Z, Xu S, Huang J. Perovskite-filled membranes for flexible and large-area direct-conversion X-ray detector arrays. Nat Photonics. 2020;14:612–7. https://doi.org/10.1038/s41566-020-0678-x.
12. Zhang Y, Liu Y, Xu Z, Ye H, Yang Z, You J, Liu M, He Y, Kanatzidis MG, Liu SF. Nucleation-controlled growth of superior lead-free perovskite Cs3Bi2I9 single-crystals for high-performance X-ray detection. Nat Commun. 2020;11:2304. https://doi.org/10.1038/s41467-020-16034-w.

13. Chen Q, Wu J, Ou X, Huang B, Almutlaq J, Zhumekenov AA, Guan X, Han S, Liang L, Yi Z, Li J, Xie X, Wang Y, Li Y, Fan D, Teh DBL, All AH, Mohammed OF, Bakr OM, Wu T, Bettinelli M, Yang H, Huang W, Liu X. All-inorganic perovskite nanocrystal scintillators. Nature. 2018;561:88–93.

14. Zhu W, Ma W, Su Y, Chen Z, Chen X, Ma Y, Bai L, Xiao W, Liu T, Zhu H, Liu X. Low-dose real-time X-ray imaging with nontoxic double perovskite scintillators. Light Sci Appl. 2020;9:112. https://doi.org/10.1038/s41377-020-00353-0.

15. Lin R, Zheng W, Zhang D, Zhang Z, Liao Q, Yang L, Huang F. High-Performance Graphene/β-Ga2O3 Heterojunction Deep-Ultraviolet Photodetector with Hot-Electron Excited Carrier Multiplication. ACS Appl Mater Interfaces. 2018;10:22419–26.

16. Xu M, Chen L, Yao Z, Ren S, Zhang Y, Huang F, Ji X, He C, Zhou L, Hu J, He S, Zhao K, Ouyang X. Transient Radiation Imaging Based on a ZnO: Ga Single-Crystal Image Converter. Sci Rep. 2018;8:4178. https://doi.org/10.1038/s41598-018-22615-z.

17. Simpson PJ, Tjossem R, Hunt AW, Lynn KG, Munné V. Superfast timing performance from ZnO scintillators. Nucl Instrum Methods Phys Res, Sect A. 2003;505:82–4. https://doi.org/10.1016/S0168-9002(03)01025-8.

18. Yamanoi K, Sakai K, Nakazato T, Estacio E, Shimizu T, Sarukura N, Ehrentraut D, Fukuda T, Nagasono M, Togashi T, Matsubara S, Tono K, Yabashi M, Kimura H, Ohashi H, Ishikawa T. Response-time improved hydrothermal-method-grown ZnO scintillator for XFEL timing-observation. Opt Mater. 2010;32:1305–8. https://doi.org/10.1016/j.optmat.2010.04.039.

19. Shimizu T, Yamamoi K, Estacio E, Nakazato T, Sakai K, Sarukura N, Ehrentraut D, Fukuda T, Nagasono M, Togashi T, Higashiya A, Yabashi M, Ishikawa T, Ohashi H, Kimura H. Response-time improved hydrothermal-method-grown ZnO scintillator for soft x-ray free-electron laser timing-observation. Rev Sci Instrum.2010;81:033102. https://doi.org/10.1063/1.3310276.

20. Armelao L, Heigl F, Jürgensen A, Blyth RIR, Regier T, Zhou XT, Sham TK. X-ray excited optical luminescence studies of ZnO and Eu-Doped ZnO Nanostructures. J Phys Chem C. 2007;111:10194–200. https://doi.org/10.1021/jp071379f.

21. Jia L, Zheng W, Huang F. Vacuum-ultraviolet photodetectors PhotoniX. 2020;1:22. https://doi.org/10.1186/s43074-020-00022-w.

22. Li Y, Zheng W, Huang F. All-silicon photovoltaic detectors with deep ultraviolet selectivity. PhotoniX. 2020;1:15. https://doi.org/10.1186/s43074-020-00014-w.

23. Zheng W, Lin R, Ran J, Zhang Z, Ji X, Huang F. Vacuum-ultraviolet photovoltaic detector. ACS Nano. 2018;12:425–31.

24. Shin HH, Joung YH, Kang SJ. Influence of the substrate temperature on the optical and electrical properties of Ga-doped ZnO thin films fabricated by pulsed laser deposition. J Mater Sci: Mater Electron. 2008;20:704. https://doi.org/10.1007/s10854-008-9788-9.

25. Khranovskyy V, Grossner U, Nilsen O, Lazorenko V, Lashkarev GV, Svensson BG, Yakimova R. Structural and morphological properties of ZnO: Ga thin films. Thin Solid Films. 2006;515:472–6. https://doi.org/10.1016/j.tsf.2005.12.269.

26. Cheng L, Zheng W, Zhu Y, Huang F, Wang H, Ouyang X. Anomalous blue shift of exciton luminescence in diamond. Nano Lett. 2022. https://doi.org/10.1021/acs.nanolett.1c04519.

27. Zhou M, Zhu H, Jiao Y, Rao Y, Hark S, Liu Y, Peng L, Li Q. Optical and Electrical Properties of Ga-Doped ZnO Nanowire Arrays on Conducting Substrates. J Phys Chem C. 2009;113:8945–7. https://doi.org/10.1021/jp901025a.

28. Chen L, He SY, Zhou LD, Huang F, Hu J, Ruan JL, Xu MX, Zhang ZB, Liu JL, Ouyang XP, Liu B. The dependence of fluorescent decay time of ZnO: Ga crystal on instantaneous non-equilibrium carriers induced by charged particles. J Lumin. 2019;214:116520. https://doi.org/10.1016/j.jlumin.2019.116520.

29. Chen L, Ruan J, Xu M, He S, Hu J, Zhang Z, Liu J, Ouyang X. Comparative study on fluorescence decay time of doped ZnO crystals under α and β excitation. Nuc Instrum Methods Phys Res Sect A: Accelerators, Spectrometers, Detectors and Associated Equipment. 2019;933:71–4. https://doi.org/10.1016/j.nima.2019.04.095.

30. Sakai E. Recent measurements on scintillator-photodetector systems. IEEE Trans Nucl Sci. 1987;34:418–22. https://doi.org/10.1109/TNS.1987.4337375.

31. Laval M, Moszyński M, Allemand R, Cormoreche E, Guinet P, Odru R, Vacher J. Barium fluoride — Inorganic scintillator for subnanosecond timing. Nucl Instrum Methods Phys Res. 1983;206:169–76. https://doi.org/10.1016/0167-5087(83)91254-1.

32. van Loef EVD, Dorenbos P, van Eijk CWE, Krämer K, Güdel HU. High-energy-resolution scintillator: Ce3+ activated LaCl3. Appl Phys Lett. 2000;77:1467–8. https://doi.org/10.1063/1.1308053.

33. Moszynski M, Kapusta M, Wolski D, Szawlowski M, Klamra W. Energy resolution of scintillation detectors readout with large area avalanche photodiodes and photomultipliers. IEEE Trans Nucl Sci. 1998;45:472–7. https://doi.org/10.1109/23.682429.

34. Yanagida T, Fujimoto Y, Yoshikawa A, Yokota Y, Miyamoto M, Sekiwa H, Kobayashi J, Tokutake T, Kamada K, Maeo S. Scintillation Properties of In Doped ZnO With Different In Concentrations. IEEE Trans Nucl Sci. 2010;57:1325–8. https://doi.org/10.1109/TNS.2009.2035120.

35. Yanagida T, Fujimoto Y, Miyamoto M, Sekiwa H. Optical and scintillation properties of Cd-doped ZnO film. Jpn J Appl Phys. 2014;53:02bc13. https://doi.org/10.7567/jjap.53.02bc13.

Publisher's Note